Materials and Structures (2009) 42:749–763
DOI 10.1617/s11527-008-9421-7

ORIGINAL ARTICLE

# Natural cement and monumental restoration

**C. Gosselin · V. Verges-Belmin · A. Royer · G. Martinet**

Received: 7 March 2008 / Accepted: 21 August 2008 / Published online: 28 August 2008


**Abstract** Natural cement, called "Roman" cement, was invented at the end of the 19th century and played an important role in the development of civil engineering works until the 1860s. More surprisingly, it was also used to restore historic buildings, such as gothic cathedrals. This paper deals with the mineralogy and the durability of natural cement in the particular case of the Bourges Cathedral in France. This study illustrates the interest of this material particularly adapted in stone repair or substitution. Contrary to traditional mortars, the present samples are made of neat cement paste, revealed by the absence of mineral additions as quartz or carbonate sand. Several combined techniques (SEM-EDS, TGA, XRD) were carried out to determine the composition of the hydraulic binder rich in calcium aluminate hydrates. The raw marl at the origin of the cement production contains oxidized pyrites which consist in a potential source of sulphate pollution of the surrounding limestone. The exposition of the cement in urban environment leads to some weathering features as atmospheric sulfation. Finally a petrophysical approach, based on water porosity, capillary sorption and compressive strength, has been performed to demonstrate the durability and the compatibility of natural cement applied as an historical building restoration mortar.

**Keywords** Natural cement · Bourges Cathedral · Mineralogy · Sulphates · Durability

C. Gosselin (✉)
Laboratory of Construction Materials (LMC), Ecole Polytechnique Fédérale de Lausannes (EPFL), Lausanne, Switzerland
e-mail: christophe.gosselin@epfl.ch

V. Verges-Belmin
Laboratoire de Recherche des Matériaux Historiques (LRMH), Paris, France
e-mail: veronique.verges-belmin@culture.gouv.fr

A. Royer
Institut National du Patrimoine (INP), Paris, France
e-mail: amandine.royer@inp.fr

G. Martinet
Laboratoire d'Etudes et de Recherches sur les Matériaux (LERM), Arles, France
e-mail: g.martinet@lerm.fr

**Notations**

| | |
|---|---|
| C | CaO |
| A | $Al_2O_3$ |
| S | $SiO_2$ |
| H | $H_2O$ |
| $\underline{C}$ | $CO_3$ |
| $ | $SO_3$ |

## 1 Introduction

Natural cements, sometimes called "Roman Cements" were discovered at the end of the 19th century in England [1, 2]. Those hydraulic binders,

originating from the calcination of marl stones, were used principally for works where rapid set and waterproof property were required. Their discovery spread quickly all over Europe, where several quarries were found out during the 19th century. Their properties made this cement of great help in buildings construction, particularly in civil engineering applications, until the development of artificial Portland cements, in the 1870s. A minor use emerged in the field of restoration of historic buildings because of specific properties of natural cement, as strong as stone, with a similar colour, but cheaper, at a time when restoration campaigns increased in scale. Some architects were also eager for experiments with new materials and techniques. Dating from 13th century and located in central France, the cathedral of Bourges is one of the best examples of the use of natural cements. The cements came from the first quarries discovered in France, in 1824 at Pouilly-en-Auxois and in 1830 at Vassy-les-Avalon (Burgundy). These cements and particularly the one from Vassy, were employed from 1824 to the 1860s, for basement waterproofing masonry, stones repointing mortar and sculpture repair [3].

The literature [4–11] reveals many scientific studies on the different materials employed in the 19th Century. The Table 1 gathers several data on the chemical composition of different natural cements, compared to limes and Portland cements. From Table 1, Vassy and Pouilly cements show a homogeneous aluminium oxide $Al_2O_3$ content close to 10% while the content of calcium and silica oxides (CaO and $SiO_2$) are more fluctuating according to the production sites. Natural cement processing required marl stones firing at temperature estimated between 1,000 and 11,00°C [3]. The variations in the oxides composition in Table 1 may originate as well as the nature of local marl banks used for the cement production than the quality of marl firing process. The other French production sites provide natural cements with a constant composition in the main oxides. Whereas $SiO_2$ and $Al_2O_3$ contents are consistent with Vassy and Pouilly ones, the significant difference resides in the CaO content, slightly lower for the other origins of natural cement. The European and US natural cements are characterized by a large dispersion in silica and calcium. These fluctuations between the European productions sites reveal an actual requirement of gathering and standardization of limes and cements composition, as initiated in France by Vicat, from 1818.

The literature mentions Portland cements as slow cements in comparison with natural cements, called rapid cements. The opposition in this nomenclature is linked to the setting time of the respective binders. Indeed Portland cement setting time is controlled by the addition of a small amount of calcium sulphate (less than five percent weight of cement is substituted by gypsum). At contrary natural cements are not added with calcium sulphate implying a very quick set. By pursuing the Table 1, Portland cements differ from natural cements by the $Al_2O_3$ content, slightly lower in the first case (from 5 to 10%) and, secondly a more controlled CaO amount (from 65 to 70%) in Portland cement.

Research into natural cements as material used in the monumental restoration is a new subject, because the use of such materials has been recently rediscovered and their historicity has been taken into account. At Bourges, the presence of natural cement on central and southern portals (Figs. 1 and 2) has been revealed the last decade [12, 13], during successive preliminary studies for the occidental facade restoration. In 2005, the French Laboratory of Research of Historical Monuments (LRMH) has worked out a scientific study of this cement applied in Bourges Cathedral [14, 15]. The characterization aimed at better understanding the composition and physical properties of the material, in order to select the most appropriate restoration product and procedure for both natural cement and adjacent stones in Bourges monument.

## 2 Sampling and experimental techniques

### 2.1 Sampling

By the end of the 20th Century, many fragments of decayed stone and mortars were about to fall on the cathedral forecourt [12]. Due to long lasting and severe stone and mortar decay, many pieces of repointing mortar and sculptures made of natural cement were removed in 2001 within the frame of a safety removal campaign. The present 11 samples were selected amongst the pieces collected during this campaign and located in the Fig. 2.

**Table 1** Chemical composition of different hydraulic binder used for construction in the XIXth Century, from [4–11]

| Nature of hydraulic binder | | Origin, plant and authors | Oxide composition (wt.%) | | | | | | |
|---|---|---|---|---|---|---|---|---|---|
| | | | CaO | $Al_2O_3$ | $SiO_2$ | MgO | FeO | $Fe_2O_3$ | $SO_3$ |
| Natural cement from Vassy and Pouilly | 1 | Vassy-les-Avallon, from Vicat [9] | 59.60 | 6.80 | 17.75 | – | – | 7.35 | 4.08 |
| | 2 | Pouilly en Auxois, from Vicat [9] | 49.60 | 10.00 | 26.00 | – | – | 5.10 | 0.69 |
| | 3 | Vassy-les-Avallon, from Claudel and Laroche [8] | 56.60 | 6.90 | 21.20 | 1.10 | 13.70 | – | – |
| | 4 | Vassy, from Debeauve [5] | 52.05 | 8.40 | 20.00 | 0.95 | 5.70 | – | 2.29 |
| | 5 | Vassy-les-Avallon, from Revue Matériaux Construction [10] | 50.90 | 9.30 | 20.30 | 0.30 | 5.50 | – | 2.86 |
| | 6 | Vassy-a, from Candlot [7] | 52.69 | 8.90 | 22.60 | 1.15 | 5.30 | – | 2.65 |
| | 7 | Vassy-b, from Candlot [7] | 50.68 | 8.76 | 23.50 | 1.80 | 5.65 | – | 3.29 |
| | 8 | Vassy-c, from Candlot [7] | 44.12 | 7.00 | 24.80 | 2.08 | 4.80 | – | 2.94 |
| | 9 | Vassy-d, from Candlot [7] | 52.20 | 9.60 | 22.40 | 1.44 | 4.76 | – | 3.13 |
| | 10 | Pouilly, from Candlot [7] | 46.10 | 10.39 | 26.80 | 1.72 | 4.61 | – | 1.42 |
| | 11 | Vassy (plant Dumarcet), from Simonet [11] | 48.06 | 10.14 | 20.26 | 0.90 | – | 4.44 | 2.87 |
| | 12 | Vassy (plant Rotton), from Simonet [11] | 46.70 | 9.64 | 20.14 | 1.10 | – | 4.86 | 2.86 |
| | 13 | Vassy (plant Faure), from Simonet [11] | 43.46 | 10.80 | 22.82 | 1.60 | – | 4.24 | 1.80 |
| | 14 | Vassy (plant Millot), from Simonet [11] | 49.90 | 10.52 | 20.10 | 1.06 | – | 4.00 | 3.18 |
| | 15 | Vassy (plant Voyot), from Simonet [11] | 46.04 | 9.66 | 21.16 | 0.97 | – | 5.12 | 2.58 |
| | 16 | Vassy (plant Prevost), from Simonet [11] | 50.14 | 9.76 | 19.74 | 1.18 | – | 4.94 | 2.89 |
| | 17 | Vassy (plant Bougault), from Simonet [11] | 49.46 | 8.76 | 19.70 | 0.86 | – | 4.98 | 3.31 |
| | 18 | Vassy (plant Détang), from Simonet [11] | 42.34 | 12.32 | 26.52 | 1.54 | – | 3.92 | 1.34 |
| Other French natural cements | 19 | L'Albarine (Ain), from Durand-Claye [4] | 47.95 | 9.25 | 23.45 | 1.45 | – | 3.83 | 0.57 |
| | 20 | Argenteuil (Seine-et-Oise), from Durand-Claye [4] | 47.50 | 8.35 | 29.55 | 3.85 | – | 4.10 | 1.10 |
| | 21 | La Bédoule (Bouches-du-Rhône), from Durand-Claye [4] | 49.05 | 11.60 | 23.45 | 1.05 | – | 4.75 | 1.02 |
| | 22 | Cahors (Lot), from Durand-Claye [4] | 50.65 | 10.75 | 28.20 | 1.05 | – | 3.50 | 1.71 |
| | 23 | Champréau (Yonne), from Durand-Claye [4] | 52.05 | 8.40 | 21.00 | 1.00 | – | 5.10 | 2.04 |
| | 24 | Chanaz (Savoie), from Durand-Claye [4] | 46.50 | 8.95 | 232.5 | 1.60 | – | 4.15 | 1.14 |
| | 25 | Chouard-Angély (Yonne), from Durand-Claye [4] | 47.70 | 12.90 | 23.40 | 1.05 | – | 3.30 | 2.69 |
| | 26 | Courterolles (Yonne), from Durand-Claye [4] | 49.15 | 9.15 | 22.15 | 0.7 | – | 5.45 | 2.00 |
| | 27 | Fresnes (Seine), from Durand-Claye [4] | 46.05 | 7.95 | 29.05 | 2.80 | – | 3.75 | 0.90 |
| | 28 | Guétary (Basses-Pyrénées), from Durand-Claye [4] | 53.80 | 8.85 | 25.10 | 1.15 | – | 3.05 | 0.94 |
| | 29 | La Valentine (Bouches-du-Rhône), from Durand-Claye [4] | 47.85 | 10.85 | 24.55 | 1.60 | – | 5.20 | 1.31 |
| | 30 | La Valentine La Méditerranée (Bouches-du-Rhône), from Durand-Claye [4] | 48.60 | 12.50 | 29.10 | 1.70 | – | 4.65 | 1.55 |
| | 31 | La Valentine Ile du Rocher Bleu (Bouches-du-Rhône), from Durand-Claye [4] | 50.45 | 11.35 | 24.65 | 1.15 | – | 5.25 | 1.02 |
| | 32 | Vimines (Savoie), from Durand-Claye [4] | 49.70 | 9.50 | 25.50 | 2.55 | – | 4.35 | 1.14 |
| | 33 | Warcq (Ardennes), from Durand-Claye [4] | 48.70 | 4.10 | 27.40 | 0.65 | – | 3.75 | 0.78 |
| | 34 | Roman cement of Boulogne, from Vicat [9] | 49.29 | 9.58 | 28.02 | 2.58 | 5.73 | – | 0.42 |

**Table 1** continued

| Nature of hydraulic binder | | Origin, plant and authors | Oxide composition (wt.%) | | | | | | |
|---|---|---|---|---|---|---|---|---|---|
| | | | CaO | $Al_2O_3$ | $SiO_2$ | MgO | FeO | $Fe_2O_3$ | $SO_3$ |
| European and US natural cements | 35 | Krienberg (D), from Michaelis, dans Wagner et al. [6] | 58.38 | 6.40 | 28.83 | 5.00 | – | 4.80 | – |
| | 36 | Sheppey (GB), from Michaelis, dans Wagner et al. [6] | 55.50 | 6.96 | 25.00 | 1.73 | – | 6.63 | – |
| | 37 | Tarnowitz (P), from Michaelis in Wagner et al. [6] | 47.83 | 1.50 | 5.80 | 24.26 | – | 20.80 | – |
| | 38 | Hausbergen (Alsace), from Michaelis in Wagner et al. [6] | 58.88 | 7.24 | 23.66 | 2.25 | – | 7.97 | – |
| | 39 | Medina Parker Nouveau, from Vicat [9] | 43.45 | 5.60 | 19.50 | 13.95 | – | 12.15 | 0.65 |
| | 40 | Zumaya (ES), from Candlot [7] | 33.04 | 7.82 | 30.80 | 0.93 | – | 5.13 | 2.37 |
| | 41 | San Sebastien (ES), from Vicat [9] | 38.34 | 17.53 | 37.65 | 0.00 | – | – | 2.73 |
| | 42 | Cumberland (US), from Candlot [7] | 36.12 | 10.66 | 29.40 | 2.42 | – | 5.37 | 1.55 |
| | 43 | Rosendale (US), from Candlot [7] | 33.02 | 7.16 | 27.50 | 19.50 | – | 4.64 | 1.09 |
| | 44 | Lehigh (US), from Candlot [7] | 48.24 | 9.12 | 24.10 | 2.42 | – | 3.18 | 1.34 |
| | 45 | Kentucky (US), from Candlot [7] | 43.40 | 4.82 | 23.00 | 12.80 | – | 3.18 | 1.81 |
| | 46 | Podolski, société Moscou, from Candlot [7] | 40.15 | 0.00 | 16.66 | 18.19 | – | 6.84 | 1.83 |
| Low hydraulic limes | 47 | Ablancourt (Marne), from Durand-Claye [4] | 59.50 | 4.90 | 12.20 | 0.90 | – | 2.50 | – |
| | 48 | Beaume (Côte-d'Or), from Durand-Claye [4] | 60.90 | 1.75 | 13.85 | 0.70 | – | 1.35 | 0.16 |
| | 49 | Les Côtes d'Alun (Haute Marne), from Durand-Claye [4] | 61.70 | 5.65 | 13.35 | 1.43 | – | 2.75 | 0.16 |
| | 50 | Malain (Côte d'Or), from Durand-Claye [4] | 65.85 | 4.45 | 10.60 | 0.50 | – | 1.35 | 0.65 |
| | 51 | Fresnes (Seine), from Durand-Claye [4] | 59.00 | 5.80 | 11.63 | 0.30 | – | 2.05 | 0.73 |
| | 52 | Les Ormes (Vienne), from Durand-Claye [4] | 64.50 | 3.05 | 9.80 | 0.80 | – | 1.30 | – |
| | 53 | Cardalou (Tarn), from Durand-Claye [4] | 67.30 | 3.60 | 13.60 | 3.20 | – | 2.35 | 0.49 |
| | 54 | Doué (Maine-et-Loire), from Durand-Claye [4] | 63.85 | 2.90 | 14.35 | 0.80 | – | 2.20 | 0.33 |
| | 55 | Echoisy La Grave (Charente), from Durand-Claye [4] | 59.20 | 4.60 | 11.70 | 1.40 | – | 2.30 | – |
| | 56 | Massay (Cher), from Durand-Claye [4] | 64.75 | 2.40 | 10.30 | 0.85 | – | 1.45 | 0.73 |
| | 57 | Les Pomets (Var), from Durand-Claye [4] | 62.40 | 4.75 | 12.15 | 0.75 | – | 1.60 | 0.57 |
| Hydraulic limes | 58 | Argenteuil (Seine et Oise), from Durand-Claye [4] | 56.80 | 5.20 | 17.85 | 1.35 | – | 2.40 | 1.06 |
| | 59 | Bar sur Seine (Aube), from Durand-Claye [4] | 59.20 | 5.20 | 17.30 | 1.90 | – | 2.60 | – |
| | 60 | La Bédoule (Bouches-du-Rhône), from Durand-Claye [4] | 58.80 | 3.45 | 16.80 | 0.85 | – | 3.45 | 0.57 |
| | 61 | Beffes (Cher), from Durand-Claye [4] | 61.35 | 4.25 | 13.50 | 1.05 | – | 3.20 | 0.37 |
| | 62 | Bougival (Seinet Oise), from Durand-Claye [4] | 57.80 | 5.00 | 16.35 | 1.00 | – | 2.10 | 0.09 |
| | 63 | Les Cordeliers (Vienne), from Durand-Claye [4] | 60.60 | 6.25 | 13.65 | 1.45 | – | 2.35 | 0.78 |
| | 64 | Cruas (Arcèche), from Durand-Claye [4] | 65.80 | 2.00 | 21.60 | 0.35 | – | 1.25 | 0.12 |
| | 65 | Saint Astier (Dordogne), from Durand-Claye [4] | 62.25 | 1.35 | 21.85 | 1.05 | – | 2.83 | 0.41 |
| | 66 | Saint Michel (Savoie), from Durand-Claye [4] | 62.20 | 5.40 | 14.20 | 2.40 | – | 2.10 | – |
| | 67 | Lafarge du Teil (Ardèche), from Durand-Claye [4] | 63.76 | 1.72 | 23.13 | 0.97 | – | 0.73 | – |

**Table 1** continued

| Nature of hydraulic binder | | Origin, plant and authors | Oxide composition (wt.%) | | | | | | |
|---|---|---|---|---|---|---|---|---|---|
| | | | CaO | $Al_2O_3$ | $SiO_2$ | MgO | FeO | $Fe_2O_3$ | $SO_3$ |
| High hydraulic limes | 68 | Albi (Tarn), from Durand-Claye [4] | 49.40 | 6.30 | 19.60 | 5.75 | – | 2.60 | 0.29 |
| | 69 | Bertaucout (Ardennes), from Durand-Claye [4] | 47.85 | 4.20 | 19.35 | 0.60 | – | 3.45 | 1.31 |
| | 70 | Chanaz (Savoie), from Durand-Claye [4] | 54.85 | 7.85 | 18.10 | 1.30 | – | 2.50 | 0.78 |
| | 71 | Charleville (Ardennes), from Durand-Claye [4] | 47.85 | 4.55 | 21.85 | 0.75 | – | 3.75 | 0.86 |
| | 72 | Chatenoy (Haut-Rhin), from Durand-Claye [4] | 57.90 | 9.25 | 21.95 | 0.25 | – | 3.20 | 0.08 |
| | 73 | Côtes d'Alun (Haute-Marne), from Durand-Claye [4] | 54.00 | 7.75 | 16.30 | 0.30 | – | 1.65 | 2.49 |
| | 74 | Sigonce (Basses-Alpes), from Durand-Claye [4] | 55.65 | 3.70 | 20.80 | 0.25 | – | 1.95 | 0.94 |
| | 75 | Virieu-le-Grand (Ain), from Durand-Claye [4] | 56.10 | 5.75 | 19.90 | 1.50 | – | 2.70 | 0.82 |
| French Portland cements | 76 | Argenteuil (Seine et Oise), from Durand-Claye [4] | 57.90 | 8.50 | 24.50 | 1.50 | – | 4.25 | 0.65 |
| | 77 | Bassin Paris (Seine), from Durand-Claye [4] | 59.80 | 9.35 | 22.30 | 1.15 | – | 3.90 | 0.41 |
| | 78 | Boulogne-sur-Mer (Pas-de-Calais), from Durand-Claye [4] | 59.40 | 7.20 | 24.10 | 0.95 | – | 3.35 | 0.43 |
| | 79 | Campbon (Loire Inférieure), from Durand-Claye [4] | 51.80 | 9.65 | 18.75 | 12.95 | – | 3.80 | 0.49 |
| | 80 | Charleville (Ardennes), from Durand-Claye [4] | 51.30 | 4.70 | 23.65 | 0.25 | – | 4.35 | 1.39 |
| | 81 | Chouard-Angély (Yonne), from Durand-Claye [4] | 49.40 | 9.05 | 22.60 | 0.90 | – | 5.95 | 2.82 |
| | 82 | Frangey (Yonne), from Durand-Claye [4] | 63.70 | 7.53 | 21.61 | 1.22 | – | 3.17 | 0.50 |
| | 83 | Marseille (Bouches-du-Rhône), from Durand-Claye [4] | 53.00 | 7.60 | 19.90 | 1.20 | – | 3.60 | 0.65 |
| | 84 | Saint-Banzille (Hérault), from Durand-Claye [4] | 60.85 | 9.55 | 22.10 | 1.30 | – | 4.25 | 0.78 |
| | 85 | Lafarge du Teil (Ardèche), from Durand-Claye [4] | 59.10 | 3.25 | 25.70 | 0.95 | – | 1.40 | 0.24 |
| | 86 | Tenay (Ain), from Durand-Claye [4] | 53.25 | 6.90 | 24.30 | 1.70 | – | 3.85 | 0.57 |
| | 87 | La Valentine (Bouches-du-Rhône), from Durand-Claye [4] | 50.45 | 8.60 | 21.25 | 2.05 | – | 4.20 | 1.35 |
| | 88 | Candlot, from Simonet [11] | 63.70 | 8.30 | 19.50 | 0.74 | – | 3.30 | 0.51 |
| | 89 | Sollier, from Simonet [11] | 64.03 | 6.03 | 22.30 | 0.97 | – | 2.94 | 0.65 |
| | 90 | Plant A, from Simonet [11] | 63.23 | 7.80 | 22.03 | 0.97 | – | 2.57 | 0.76 |
| | 91 | Couronne, from Simonet [11] | 64.33 | 6.26 | 21.70 | 1.10 | – | 2.47 | 0.71 |
| | 92 | Darsy, from Simonet [11] | 60.35 | 9.30 | 21.35 | 0.90 | – | 2.30 | 0.98 |
| | 93 | Cambier, from Simonet [11] | 63.05 | 7.80 | 20.75 | 0.75 | – | 3.03 | 0.61 |
| | 94 | Delbende, from Simonet [11] | 63.40 | 8.30 | 21.07 | 1.10 | – | 2.47 | 0.54 |
| | 95 | Cie Nouvelle, from Simonet [11] | 62.68 | 8.32 | 22.00 | 0.80 | – | 2.23 | 0.53 |
| | 96 | Plant B, from Simonet [11] | 62.95 | 8.15 | 22.05 | 0.85 | – | 2.40 | 0.74 |
| | 97 | Quillot, from Simonet [11] | 64.00 | 8.30 | 20.00 | 1.65 | – | 2.15 | 0.29 |

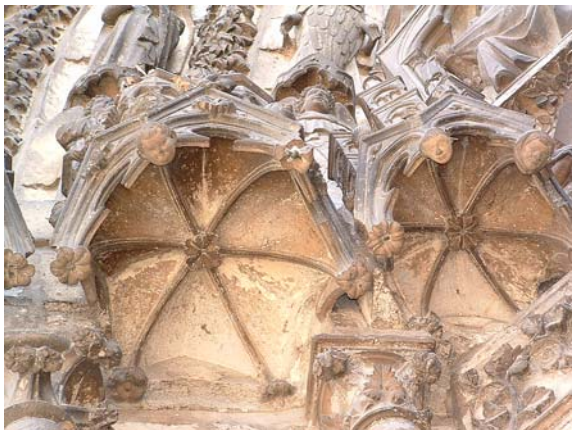

**Fig. 1** Head and flower shape ornamentations made in natural cement, under a dais (cl. C. Gosselin [14]). In the center, apparent iron bar shows the sealing system using plaster

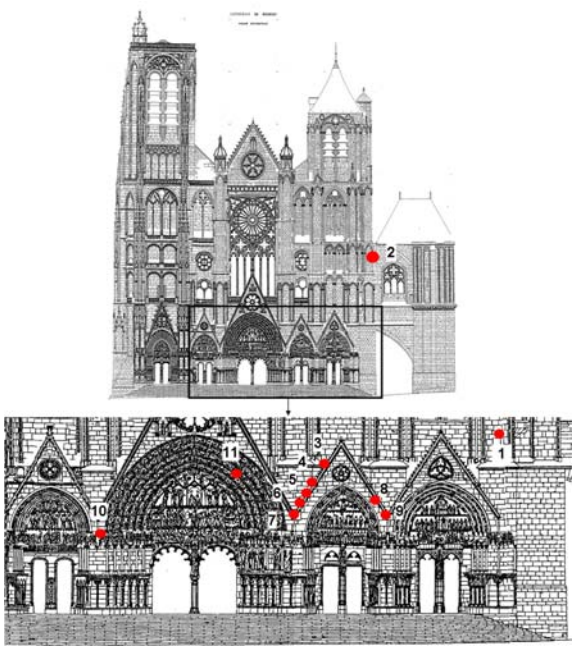


**Fig. 2** Location of samples on the cathedral occidental façade (scheme from Société Française de Stéréotopographie 1969). The view of central and southern portals is detailed to locate the samples

Sample 1 (Fig. 3a) is a fragment of a repointing mortar while samples 3–11 come from ornamentation sculptures standing on the third portal gable (Fig. 3b) or on the central portal vaults (Fig. 3c). Only one sample of limestone (sample 2) comes from a hook shaped sculpture.

## 2.2 Experimental techniques

The present experimental procedures are inspired from the literature on historical mortars characterization [16–19]. Preliminary phenolphthalein (concentration 1%) was pulverized on freshly fractured samples to distinguish carbonated from non carbonated areas. The latter were then preferentially studied mineralogy of the cementitious matrix because their content of calcium carbonate is lesser [20].

Mortar macrostructure was observed on thin and polished sections, using natural or polarised reflected light optical microscopy (Leica DM) equipped with digital camera.

The microstructure was observed by scanning electron microscopy (JEOL JSM 5600 LV) and analysed by electron probe microanalysis. Backscattered electron technique (Low Vacuum 17 Pa, 15 kV acceleration voltage) on polished sections was used for elementary chemical analysis. Secondary electron imaging, on carbon coated fresh fractures (High Vacuum, 25–30 kV acceleration voltage), provided high resolution images of the microstructure morphology.

Crystallized phases were determined by X-ray diffraction, using a Brücker D8 Advance diffractometer (100 µm sieved fraction powder method, Cu tube, $2\theta = 5$–$65°$) with long time acquisition parameters (step size = 0.01°, step time = 10 s, rotation speed = 10 rpm).

A complementary mineralogical analysis was performed by the LERM in Arles. This includes a chemical analysis of the acid soluble fraction ($HNO_3$ 1:50) according to the protocol described in [18]. A complementary thermogravimetric/differential thermal analysis (TGA/DTA Netzsch), until 1,000°C and under $N_2$ atmosphere is used. These coupled methods aim at determining the mineralogical composition of the mortar. The computation principle is based on oxides Bogue calculation and the results are expressed in weight percent of binder, aggregate and carbonated fraction [21]. This qualitative and quantitative approach, usually known as "Calcul Mineraux LCPC" method, was applied only on sample 8.

The separation of aggregates from hydraulic binder was performed using diluted (1:3) HCl acid etching [16]. After etching, the filtrate was rinsed with distilled water, dried and weighted before optical observation and XRD analysis.

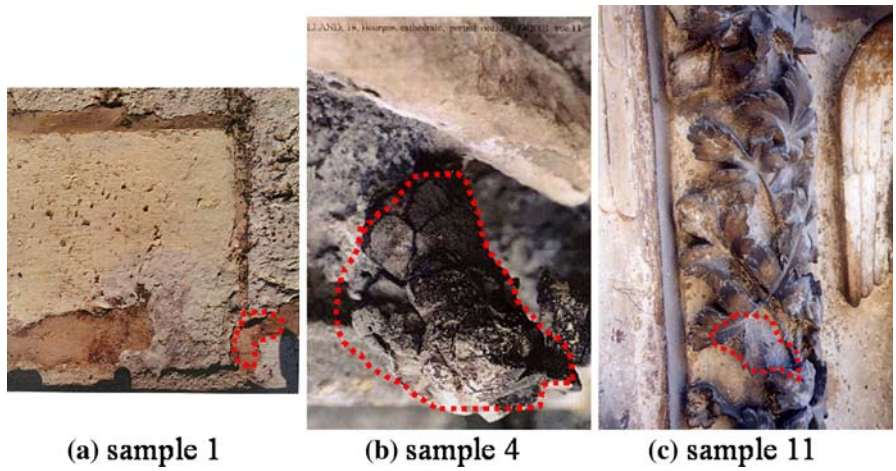


**Fig. 3** Different natural cement applications on the cathedral: (**a**) stone repointing (cl. O. Rolland [12]), (**b**) hook shaped sculpture (cl. O. Rolland [12]), (**c**) leaf shaped sculpture

Petrophysical characterization of cement and limestone has been comparatively done on parallepipedic specimens. The total porosity $N_t$, the 48 h porosity $N_{48}$ and the kinetics of capillary rise were measured according to the RILEM recommendations [22].

Finally compressive strength tests were performed using an Instron 5500R hydraulic press, and managed at a controlled displacement rate of 0.5 mm/min.

## 3 Results

### 3.1 Macroscopic observations

Cement samples present common weathering forms, such as from biological colonization (lichens, mosses) or black crusts, as a signature of rich sulphur urban atmosphere on calcareous materials [23]. Some samples present a network of deep cracks but no corrosion products have been observed, especially in the casting marks of the copper sealing rebars.

The samples present an original aspect and show a very fine, beige coloured and homogenous texture. In most cases a sub-millimetre thick brownish oily-aspect layer underlines the surface, as previously observed by Weber [24] on roman cement mortars sampled from European monuments. Traditional repair mortars contain mineral additives (sand, stone powder, pozzolans and/or tile fragments) but the matrix of our samples does not contain any of these coarse inclusions. Given these preliminary observations, all available specimens seem to come from the same restoration campaign. While the general texture looks similar for every sample, some nuances of colour are distinguishable in the matrix. After pulverising phenolphthalein solution on fresh fracture, this difference coincides with carbonated and non carbonated areas.

### 3.2 Microstructure

The microstructure has been investigated using optical and scanning electron microscopy on thin and polished sections. From optical examination the matrix is composed of a binder including distinct and small inclusions. The porosity is defined by spherical and oblong pores with a large range of sizes, from 50 μm to 1 mm, and with a mean diameter estimated at 200 μm. The few microcracks, probably originating from preparation artifacts, are isolated and do not constitute a well defined network.

Optical microscopic exams are performed on polished sections etched by borax. This etching method reveals the major mineral phases like clinker grains not reacted with water during or after the mixing of mortar. Figure 4 shows two types of anhydrous grains of cement (50–200 μm size) present in the matrix. The first type of encountered cement grains, illustrated in Fig 4a, is composed of blue to brown spherical and oblong particles in a white matrix. These spherical particles represent mainly dicalcium silicate grains ($C_2S$) contained in a white colored solid solution composed of calcium-aluminates such as tetra-calcium-alumino-ferrite ($C_4AF$) [25, 26]. The second type of anhydrous clinker grain is illustrated in Fig. 4b. These grains are only composed of calcium-aluminates such as tricalcium-aluminates ($C_3A$, grey

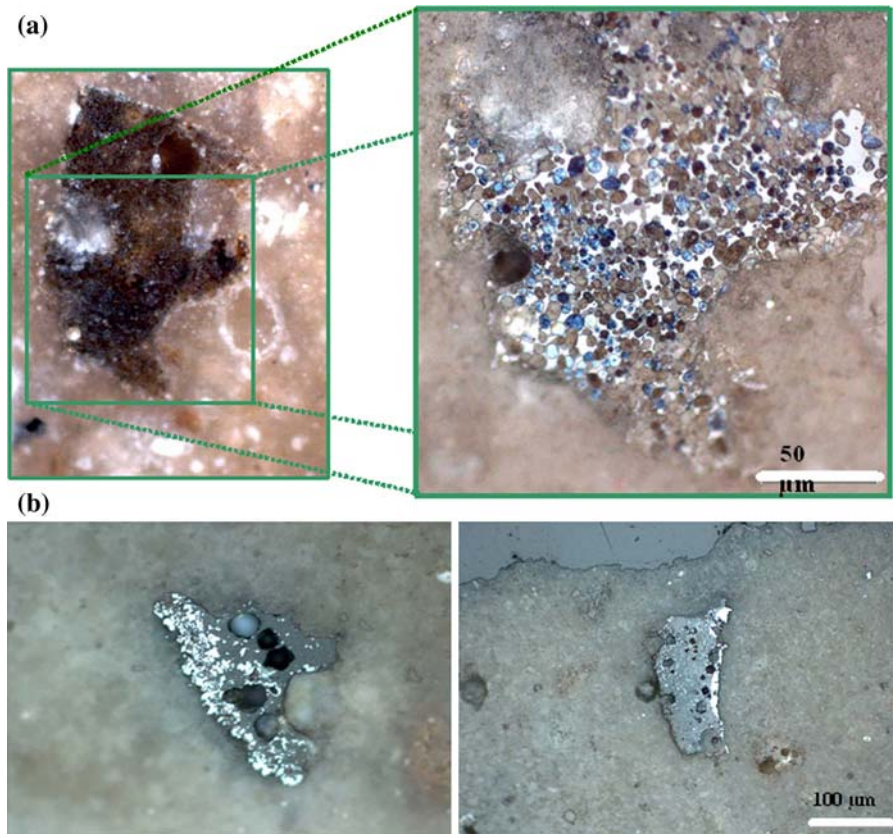


**Fig. 4** Photomicrograph of anhydrous grains of clinker on etched polished section. (**a**) Reflected natural light (left) and reflected polarized light (right) to show (blue brown) $C_2S$ grains in a (white) rich $C_4AF$ matrix. (**b**) Reflected polarized light view (grey) $C_3A$ and (white) $C_4AF$ rich grains clinker

coloration) or tetra-calcium-alumino-ferrite ($C_4AF$, white coloration).

The rarity of clinker grains in the matrix proves the high degree of hydration of the cement. The heterogeneous nature and form of clinker grains could originate from a non optimized process of marls firing. Indeed kiln temperature must be constant to obtain a homogeneous composition of clinker.

### 3.3 Analysis of aggregates

Optical microscopy examination of thin sections confirmed the naked eye observations on the absence of quartz sand or stone fragments in the mortar. As a complementary investigation, we proceeded to an acid etching of bulk mortar allowed to separate siliceous inclusions from the binder. Filtrate residue (which represents 12–15% of bulk mortar mass) is composed of fine grains (5–10 µm) or grains groups (20–50 µm). XRD analysis gives the following crystallographic nature of these grains: quartz $SiO_2$, tridymite $SiO_2$ and goethite FeOOH.

### 3.4 XRD analysis

The main crystallized phases of the samples are detected by XRD and the results are resumed in Table 2.

As mentioned above, calcite and vaterite are the two major phases detected in carbonated samples. Among the main crystalline phases characterizing the binder, calcium silicate hydrate is a long term hydration product of $C_2S$, known to be slowly reactive. Then $C_4AH_{13}$ is a member of hydrocalumite minerals and results from the hydration of calcium aluminates, such as $C_3A$ grain observed on thin sections. This reaction is favored in presence of Portlandite CH [27]. The latter, undetected by XRD, seems to be weakly crystallized even within non carbonated samples. Nevertheless, SEM-EDS examinations reveal the presence of CH in very small pores (Fig. 5).

Hydrogarnet $C_3AH_6$ is a stable phase corresponding to the complete thermodynamical conversion of $C_4AH_{13}$. Finally ettringite and gypsum indicate a

**Table 2** Results of XRD semi quantitative analysis of carbonated and non carbonated (7 and 8 in bold) samples: significant (+++), average (++), weak (+), trace (t) conformity of diffraction peaks versus reference file

| | Carbonated samples | | | | | | | | Non carbonated samples | |
|---|---|---|---|---|---|---|---|---|---|---|
| | 1 | 3 | 4 | 5 | 6 | 9 | 10 | 11 | 7 | 8 |
| Calcite CC | +++ | +++ | +++ | +++ | +++ | +++ | +++ | +++ | ++ | ++ |
| Vaterite CC | ++ | ++ | ++ | ++ | ++ | ++ | ++ | ++ | – | – |
| Quartz $SiO_2$ | ++ | ++ | ++ | ++ | ++ | ++ | ++ | + | + | + |
| Calcium silicate hydrate $C_2SH_{0.5}$ | – | – | – | – | – | – | – | – | ++ | ++ |
| Hydrogarnet $C_3AH_6$ | – | – | – | – | – | – | – | – | ++ | + |
| Hydrocalumite $C_4AH_{13}$ | – | – | – | – | – | – | – | – | ++ | ++ |
| Gypsum C$H$H$_2$ | + | + | + | + | – | t | t | + | ++ | +++ |
| Ettringite $C_3A \cdot 3C\$H_{32}$ | – | – | – | – | – | – | – | – | +++ | + |

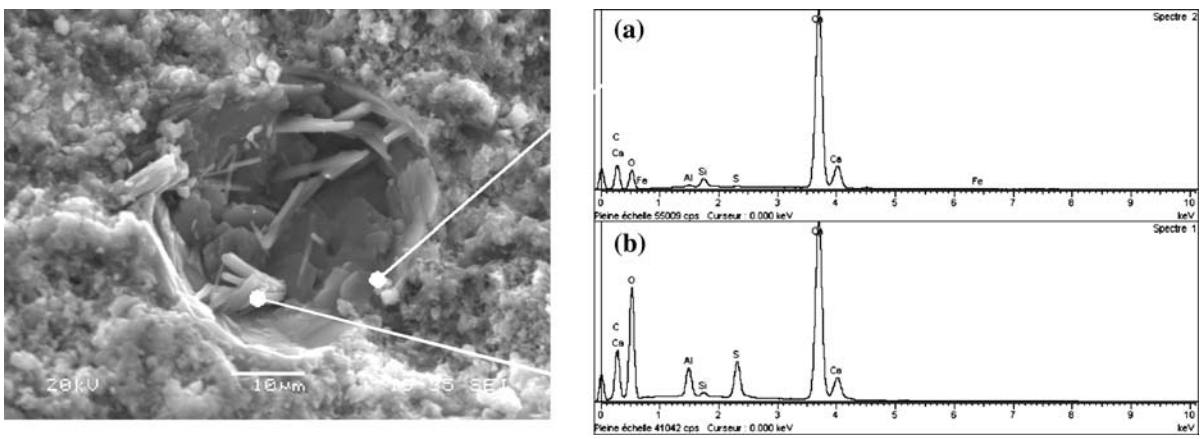


**Fig. 5** SEM-EDS analysis of a pore recovered by portlandite (EDS spectrum a) and ettringite needles (EDS spectrum b)

reaction between sulphates and the calcareous binder as commented below.

### 3.5 TGA/DTA results

The TGA/DTA results are given in Table 3. This method allows the quantification of hydrated phases and calcium carbonate, for which the thermal decomposition corresponds to distinct ranges of temperature. In the case of sample 8, 15.6% of mass is attributed to hydrated phases (ettringite and calcium aluminate hydrates) and 12.7% is related to calcium carbonate.

### 3.6 Chemical composition

The nitric acid etching of sample 8 confirms that the mortar contains a low amount of insoluble fraction (7%). The analysis of soluble fraction, expressed in wt.% of oxides is resumed in Table 3. The high loss on ignition could confirm the high degree of carbonation but as well the high degree of hydration of the cement. By combining chemical and thermal results, a calculation is carried out to approximate initial mortar composition: hydraulic binder 60.2%, siliceous fraction 7.0% and carbonate fraction 30.5%. Concerning the siliceous fraction, this composition corresponds to the preliminary observations of insoluble residue after HCl (1:3) etching and confirms the presence of quartz only in raw marl stones. Concerning the carbonated fraction, results of mineral computation have to be taken into account carefully. Indeed, this method is limited for highly carbonated materials because the distinction between calcite of calcareous aggregates and matrix carbonation is impossible at this stage of investigation. Moreover,

**Table 3** Thermal analysis (bound water and decarbonation) of the bulk sample 8 and chemical analysis (expressed in wt.% of oxides) of it soluble fraction after nitric etching

| | Elements | Wt.% |
|---|---|---|
| Thermal analysis | Free water (<60°C) | 0.2 |
| | Bound water (60–550°C) | 15.6 |
| | From ettringite | 3.3 |
| | From hydrated aluminates | 6.1 |
| | Loss for 550–1,000°C | 12.7 |
| | $CO_2$ from calcite | 11.6 |
| | Corresponding calcite | 26.4 |
| | Total loss | 28.4 |
| Chemical analysis | $SiO_2$ | 13.83 |
| | $Al_2O_3$ | 5.49 |
| | $Fe_2O_3$ | 2.13 |
| | CaO | 40.87 |
| | MgO | 0.94 |
| | $SO_3$ | 1.48 |
| | $P_2O_5$ | 0.16 |
| | $Na_2O$ | 0.04 |
| | $K_2O$ | 0.10 |
| | $TiO_2$ | 0.14 |
| | MnO | 0.19 |
| | $Cr_2O_3$ | 0.01 |
| | SrO | 0.06 |
| | Cl | 0.01 |
| | Insoluble fraction | 6.15 |
| | Loss ignition | 28.40 |
| | Total | 100.00 |

the calcareous fraction could also correspond to incompletely burnt marl fragments. Nevertheless, no typical calcite grains, coming from hypothetical limestone aggregates, have been observed on thin section.

Table 3 shows high content of $SO_3$ in the binder composition. Sulphates are linked to the presence of ettringite and gypsum (Table 2 and Sect. 3.7) but also unfired marl blocks or combustibles used for cement production. From Table 1, among all French natural cements, Pouilly but especially Vassy cements contain a high amount of sulphate, with an average of 2.8% $SO_3$. Furthermore, $SO_3$ content is much higher than the one of French Portland cements (0.75%) and hydraulic limes (0.48, 0.48 and 0.94% respectively for low, medium and high hydraulicity).

### 3.7 Source of sulphates

The hydrated phases containing sulphur are significantly detected as gypsum and ettringite. Those two phases are secondary formations coming from the effect of sulphur or sulphates sources on calcium and aluminium hydrates phases of cement. Gypsum is present as well as in bulk mortar (XRD results) than on external subsurface (revealed by elemental EDX mapping of Ca and S, performed on polished sections where the external border is covered with a thin black crust). Ettringite is mainly observed in the pores of the matrix and presents different degrees and forms of crystallization.

Concerning the internal sources of sulphur, several grains of pyrite (iron sulphur $FeS_2$) have been observed enclosed in the cement matrix. Pyrites originate from the raw marl stones used for the cement process. Figure 6 displays a grain of oxidized pyrite using optical microscopy (left) and corresponding SEM image (right). X-Ray mapping illustrates the repartition of iron Fe, sulphur S and oxygen O in such oxidised pyrite grain. More generally, the pyrites observed under SEM present different degrees of oxidation.

### 3.8 Petrophysical and durability properties

Comparative petrophysical tests have been performed on cement mortars and limestone specimens to measure the porosity, the capillary sorption and evaluate the properties of fluid transfers within each material and at their interface. This characterization evaluates the compatibility of natural cement applied as a repair material on a calcareous substrate. Table 4 gives results of cement and limestone samples presenting appropriated dimension to prepare prismatic specimens.

The amount of water absorbed in a given time, by dried samples with rectangular section and in contact with free water surface, follows the relation $m = A\ t^{1/2}$, where $m$, the amount of water (g cm$^{-2}$) and $t$, time. The constant $A$ is called water absorption coefficient (kg m$^{-2}$ h$^{-1/2}$). Simultaneous measurement of water level raised by capillarity is operated to determine the rate of water sorption following the relation $h = B\ t^{1/2}$, where $h$ is height of water uptake, $B$ the water sorption rate (g cm$^{-2}$) and $t$ time. $N_t$ and $N_{48}$ are defined as the amount of water absorbed

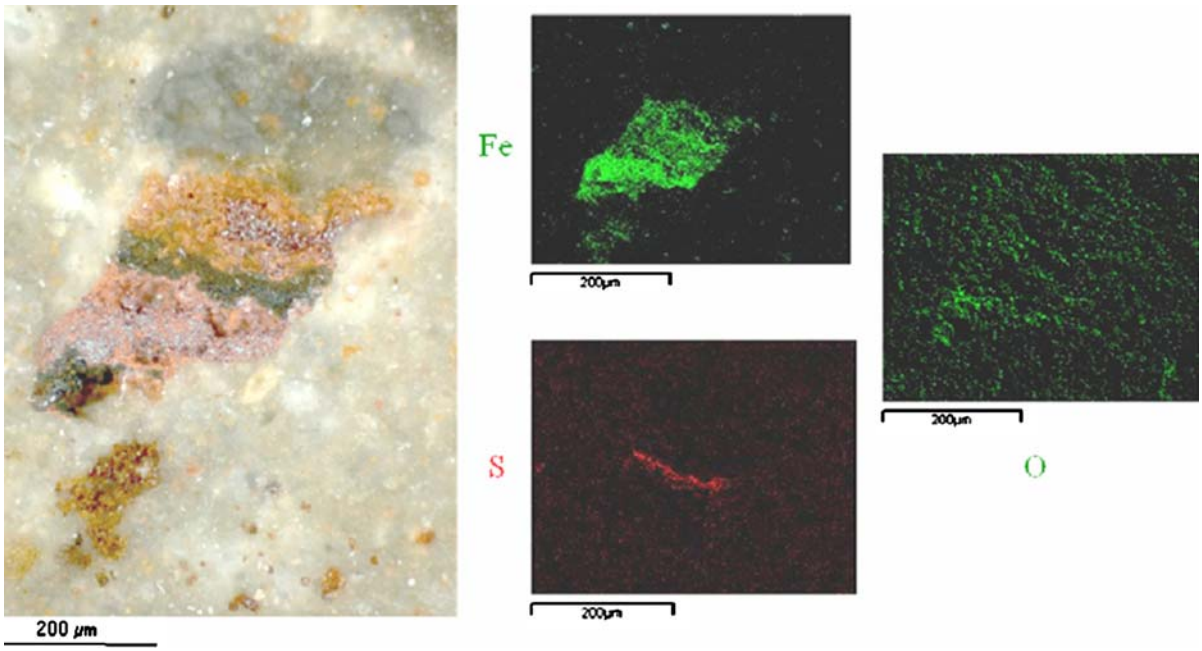


**Fig. 6** Grain of oxidised pyrite. Left: Reflected natural light OM exam to see rusty aspect of oxidised pyrite in cement. Right: X-ray mapping of the same grain to show repartition of iron, sulphur and oxygen

under vacuum respectively during 24 and 48 h. The ratio between $N_t$ and $N_{48}$ is called as Hirschwald coefficient $S_{48}$.

The solid density of all cement specimens is homogeneous while the bulk density differs significantly. The fluctuations in water/cement ratio used during the preparation of the cement paste are involved in the variation of the bulk density. Furthermore, the cement specimens present a higher total porosity (25–30%) than limestone ones (15–20%). Capillary sorption results reveal that cement matrix presents a water sorption capacity and kinetic coefficients significantly higher than calcareous substrate. This tendency is convenient in term of hygroscopic transfers between the two materials. High capillary sorption within the mortar avoids the water retention, especially at the interface stone/mortar and limits the risks of damaging salts crystallisation.

Table 4 gives compressive strength results measured on the most porous sample of cement mortar (sample 10). The mean compressive strength reaches 15 MPa with a low standard deviation (1.7 MPa). Comparatively six months compressive strength has been evaluated in 1903 by the Laboratoire de la Ville de Paris [10] on different samples of Vassy cements coming from several plants (Table 5). Those results were measured on neat cement paste (equal part of water and cement, without sand). By comparing these 6 months strength to longer term the ones at around 160 years (17.6 MPa), we can conclude that the roman cement, mixed and applied in those conditions, would have passed through time without any loss of strength. This conclusion, based on petrophysical properties of a porous sample (50%), could well be drawn to all natural cement specimens present on the façade of the edifice.

## 4 Discussion

At Bourges, the natural cement mortar is distinguished from traditional ones by the absence of mineral admixtures such as siliceous and carbonates aggregates. The insoluble residue size is such small that any addition of siliceous aggregates can be considered. This indication highlights a deficiency on the mix design.

Indeed the use of pure cement paste can promote successively thermal and mechanical shrinkage. This is confirmed by the archives mentioning a premature cracks network on mortar surface, only two years after the end of the works [3].

**Table 4** Capillary water uptake, water porosity, and density on limestone (†) and roman cement (*) specimens (complemented with compressive strength of cement sample 10)

| Sample | Value A (kg $m^{-2}$ $h^{-1/2}$) and correlation $R^2$ | Value B (cm $h^{-1/2}$) and correlation $R^2$ | $N_t$ (%) | $N_{48}$ (%) | Hirschwald coefficient ($S_{48}$) | Bulk density (g $cm^{-3}$) | Solid density (g $cm^{-3}$) | Ultimate compressive strength (MPa) |
|---|---|---|---|---|---|---|---|---|
| 1-1* | – | – | 28.62 | 20.10 | 0.70 | 1.80 | 2.52 | – |
| 2-a† | – | – | 16.31 | 15.00 | 0.92 | 2.28 | 2.72 | – |
| 2-b† | 1.07 ($R^2 = 0.9835$) | 1.04 ($R^2 = 0.998$) | 14.41 | 15.49 | 0.93 | 2.28 | 2.69 | – |
| 2-c† | 0.45 ($R^2 = 0.9984$) | 0.71 ($R^2 = 0.980$) | 17.93 | 16.47 | 0.92 | 2.19 | 2.67 | – |
| 2-d† | 0.78 ($R^2 = 0.9907$) | 0.61 ($R^2 = 0.994$) | 20.67 | 18.75 | 0.91 | 2.28 | 2.88 | – |
| 2† | – | – | 19.88 | – | – | 2.14 | 2.66 | – |
| 3* | – | – | 24.78 | – | – | 1.86 | 2.47 | – |
| 4-a* | – | – | 27.24 | – | – | 1.80 | 2.48 | – |
| 4-b* | – | – | 30.01 | – | – | 1.70 | 2.43 | – |
| 10-a* | 8.56 ($R^2 = 0.999$) | 2.32 ($R^2 = 0.989$) | 49.86 | 49.10 | 0.96 | 1.32 | 2.63 | 15.34 |
| 10-b* | 9.25 ($R^2 = 0.999$) | 2.38 ($R^2 = 0.989$) | 48.21 | 46.46 | 0.96 | 1.34 | 2.59 | 12.88 |
| 10-c* | 9.03 ($R^2 = 0.998$) | 2.50 ($R^2 = 0.994$) | 47.24 | 45.36 | 0.96 | 1.39 | 2.63 | 15.50 |
| 10-d* | – | – | 48.01 | 46.37 | 0.97 | 1.35 | 2.60 | 17.17 |
| 10-e* | – | – | 49.23 | 47.20 | 0.96 | 1.33 | 2.63 | – |
| 11* | – | – | 27.46 | – | – | 1.78 | 2.46 | – |

**Table 5** Six months compressive strength results on Vassy cement paste coming from several plants, from [10]

| Vassy cement plant | Pure paste compressive strength (MPa) |
|---|---|
| Bougault | 18.30 |
| Dumarcet | 20.50 |
| Faure | 17.58 |
| Millot et Cie | 16.58 |
| Prévost | 16.80 |
| Rotton | 17.00 |
| Voyot | 16.42 |
| Mean | 17.60 |

The quartz and tridymite present in the insoluble residue led us to raise some questions on the temperature of marl stones calcination. During this process, $\alpha$-quartz undergoes successive transitional phases: $\beta$-quartz at 573°C, (minor, short and unstable phase), tridymite (unstable phase between 867 and 1,450°C) and cristobalite (stable phase above 1,450°C) [27]. Moreover, according to the literature, natural cement process required marls firing at temperature estimated between 1,000 and 1,100°C [3]. Within this range of temperature, only tridymite would be present in the insoluble residue. The simultaneous presence of very fine grains of tridymite and quartz in the samples shows a heterogeneous firing of marl blocks. Consequently quartz originates from unfired marl fragments while tridymite is a residue of completely burnt stones.

The presence of incompletely burnt marl stones reflects the heterogeneity of calcination temperature, directly linked to weakly optimized process of firing. The use of shaft kiln was probably the main reason of such fluctuations in the cement production. From 1824, the development of Portland cements [28] had undergone similar defaults in the process of fabrication. Through the nineteenth Century, successive improvements in cement industry resulted, from the late 1870s, in the continuous production using rotary kiln and ball milling to grind the cement.

The main anhydrous phase of the natural cement of Bourges is a bicalcium silicate $C_2S$, obtained for a temperature range of 900–1,100°C. Above this temperature, tricalcium silicates $C_3S$ would be the main reactant of the cement. The absence of $C_3S$ confirms thus the data from the literature [3] on the cement calcination (1,000–1,100°C). At this range of temperature, the formation of $C_4AF$ and $C_3A$ depends on the sufficient amount of $Al_2O_3$ and $Fe_2O_3$ in marls before it calcination. According to the literature [4–11], global chemical analysis of Vassy cement give

9.20% and 5.58% respectively for $Al_2O_3$ and $Fe_2O_3$ amount, allowing the formation of significant amount of $C_4AF$ and $C_3A$ in the clinker.

The determination of hydrated phases details the nature of raw marl used for the cement production. Vicat estimated a minimum clayey fraction of 27–30% in marl stones destined to natural cement production [9]. In Bourges cement, highly argillaceous limestone is exhibited by a binder rich in calcium aluminates hydrates. $C_4AH_{13}$ is clearly detected and partially converted into stable form $C_3AH_6$. The binder rich in calcium aluminate confers to the material a high reactivity and rapid setting time. These properties are generally linked to a great heat of hydration and a consequent thermal shrinkage, as mentioned above. Additionally to calcium aluminate phases, poorly crystalline CSH suggests the hydration of $C_2S$.

The chemical and mineralogical results retain attention on the high amount of sulphur in the cement samples. The influence of sulphur on Vassy cement has been notified from the earliest applied chemistry handbooks [4]. In 1885, Durand-Claye discussed the quality of those cements despite of their good hydraulic index—i.e. as defined by Vicat in 1856, the ratio between oxides from clay and lime fractions in raw marls, $i = (SiO_2 + Al_2O_3)/CaO$. Earlier in 1857, Vicat [29] attributed the high sulphur content to accidental presence of calcium sulphate coming from sedimentary marls layer or combustibles used for cement manufacture. This initial sulphate content was qualified as defect by Vicat and the concerned cements were avoided for marine structures, subject to aggressive saline environment.

In the present samples, the combination of sulphur and calcium on the subsurface results typically from a sulphation of hydrated phases (CH, $C_4AH_{13}$), anhydrous grains ($C_3A$), or calcium carbonate, by soluble atmospheric $SO_2$. The mechanisms of calcareous stones are well identified [23] but the atmospheric sulphation of mortars and concretes need more understanding. Recent studies [30] have explored the process of concrete sulphation by sulphur dioxide in urban and industrial sites. This type of sulphate attack in such conditions promotes mainly the formation of gypsum and ettringite in the porosity and the matrix of cementitious materials. Ettringite is thus a product of reaction between gypsum and anhydrous cement grains (such as $C_3A$ and $C_4AF$) or hydrated calcium aluminates phases ($C_4AH_{13}$). Depending on the concentration of available sulphates and calcium aluminates, ettringite can expand with high pressure of crystallization generating internal mechanical strength. In particular conditions (location of ettringite growth, space availability), this pressure can lead to damage of the cement matrix.

Additionally to atmospheric soluble $SO_2$, plaster, applied to seal natural cement pieces [3, 12], is an external source of $SO_3$.

The oxidized pyrites implicate an internal source of sulphate, originating from raw marl to process the cement. Originally the alteration of pyrites in marls can occur from a sedimentary process. This hypothesis would imply that goethite FeOOH, product of pyrite oxidation and identified in the acid insoluble fraction, should have been totally decomposed during the calcination stage and transformed into hematite $Fe_2O_3$ from a temperature of 250°C. Consequently the presence of FeOOH corresponds to a secondary alteration occurring beyond the cement production or hydration. In this case, sulphuric acid released from pyrite alteration would react with calcium aluminates of the binder to produce gypsum and ettringite [31]. However such reaction rims have not been observed in the surrounding of pyrite grains.

The two sources of sulphates (external from atmospheric $SO_2$ and internal from oxidized $FeS_2$) figured out in this study are potential sources of limestone pollution, when solubilised sulphates migrate to the calcareous matrix. Recent works [32], based on the dosage of sulphur and oxygen stable isotopes, have been currently carried out to characterize the different sources of sulphates in Bourges cathedral samples (healthy or decayed stone, plaster, roman cement). This isotopic approach aims at comparing the sulphatic signature of cement with the sulphates present in decayed stones, in order to evaluate the potential of pollution of natural cement on the edifice stones.

Although the natural cement used in Bourges constitutes a potential source of sulphates due to the high level of pyrites oxidation, its compatibility with limestone has been is clearly demonstrated. The high porosity and the possibility of water to evaporate characterize the natural cement as particularly adapted to substitute and repair the stones, in respect with proper fluids transfers and prevention of sulphate salts crystallisation.

## 5 Conclusions

This article gives new results on the characterization of natural cements produced in France during the 19th century. Their special application in monumental stones restoration is studied by the mean of mineralogical and petrophysical approaches. Through the determination of the cement composition and durability properties, the knowledge on natural cement process (nature of clayey marls stones, calcination temperature) and the state of art of stone restoration is enhanced. As the most of calcareous materials exposed in urban environment, natural cements undergo atmospheric sulfation leading to it superficial weathering (black crust). The several grains of oxidized pyrites have been identified as an internal source of sulphate. The soluble sulphates can react with calcium aluminate phases of the cement to form ettringite and gypsum. A secondary reaction involves the soluble sulphates migration through the cement to the calcareous substrate, leading to potential damage of the edifice stones. On one hand, the salt migration could be promoted by the high porosity of the cement matrix. But on the other hand, the high porosity and capillary transfer of the cement allow the evaporation of water and the crystallization of salt at the interface cement–stone. This property, complemented with consistent long term compressive strength, demonstrates the durability and the compatibility of natural cement to restore monumental stones.

**Acknowledgements** This study is a part of the French National Research Program on Knowledge and Conservation of Materials of Cultural Heritage financed by DRAC Centre, Research Division of BRGM and the Musée du Chateau de Versailles. M. O. Rolland, sculptures restorer, is acknowledged for his help in samples inventory and his knowledge of this roman cement applied in Bourges Cathedral. M. E. Cailleux, LRMH, is acknowledged for his help on the characterization of the natural cement.

## References

1. Hughes DC, Sugden DB, Jaglin D, Mucha D (2008) Calcination of Roman cement: a pilot study using cement–stones from Whitby. Construct Build Mater 22(7):1446–1455. doi:10.1016/j.conbuildmat.2007.04.003
2. Hughes DC, Swann S, Gardner A (2007) Roman cement: part one: its origins and properties. J Archit Conserv 13(1):21–36
3. Royer A (2006) Le ciment romain en France: un matériau du XIXe siècle méconnu. Monumental, pp 90–95
4. Durand-Claye CL (1885) Chimie appliquée à l'art de l'ingénieur. In: Encyclopédie des travaux publics. Baudry et Cie, Paris
5. Debauve A (1886) Procédés et Matériaux de Construction tome 3. Dunod et Vicq, Paris
6. Wagner R, Fischer F, Gautier L (1903) Traité de Chimie Industrielle tome 2. Masson, Paris
7. Candlot E (1906) Ciments et chaux hydrauliques. Fabrication Propriétés Emploi, 3rd edn. Paris et Liège, Paris
8. Claudel J, Laroque L (1850) Pratique de l'Art de Construire. Maçonnerie. Carilian-Goeury et Vor Dalmont, Paris
9. Vicat LJ (1856) Traité pratique et théorique de la composition des mortiers, ciments et gangues à pouzzolanes et de leur emploi dans toutes les sortes de travaux, suivi des moyens d'en apprécier la durée dans les constructions à la mer. Grenoble
10. Le ciment de Vassy (1905–1906) Revue des Matériaux de Construction et de Travaux Publics. Margry, Paris, pp 290–292
11. Simonet E (1897) Maçonneries. Librairie des Ponts et Chaussées, des Mines des Chemins de Fer. Dunod et Vicq, Paris
12. Rolland O (2001) 18, Bourges, Cathédrale, portail occidental, rapport de relevé de fissures et de mise en sécurité'. Direction régionale des affaires culturelles de la région Centre, Orléans, Unpublished report, 113 pp
13. Di Matteo C (1992) Etudes et essais de traitement des sculptures de la cathédrale de Bourges. In: CNRS Editions, La conservation de la pierre monumentale en France. Paris, 272 pp
14. Gosselin C (2005) Le ciment romain: une source potentielle de sulfates dans la dégradation des pierres de la Cathédrale de Bourges. Master Thesis, University of Paris, Unpublished report, 62 pp
15. Verges-Belmin V, Gosselin C (2006) Le ciment romain: une source potentielle de sulfates dans la dégradation des pierres de la Cathédrale de Bourges. Monumental, pp 96–99
16. Callebaut K (2002) State of the art of research/diagnostics of historical building materials in Belgium. In: Advanced Research Centre for cultural heritage interdisciplinary projects. Fifth Framework Programme Workshop, Prague
17. Palomo A, Blanco-Varela AMT, Martinez-Ramirez S, Puertas F, Fortes C (2002) Historic mortars: characterization and durability. New tendencies for research. In: Advanced Research Centre for cultural heritage interdisciplinary projects. Fifth Framework Programme Workshop, Prague
18. Martinet G, Quénée B (2000) Proposal for a useful methodology for the study of ancient mortars. In: RILEM, International RILEM workshop on historic mortars: characteristics and tests. Paisley, pp 81–93
19. van Hees RPJ, Binda L, Papayianni I, Toumbakari E (2004) Characterisation and damage analysis of old mortars. Mater Struct 37:644–648. doi:10.1007/BF02483293
20. Baroghel-Bouny V (1994) Caractérisation des Pâtes de Ciment et des Bétons. Méthodes, Analyses, Interprétations. LCPC, Paris
21. Deloye FX (1991) Le calcul minéralogique: application aux monuments anciens. Bulletin de Liaison LCPC 175:59–65

22. RILEM (1980) Recommended tests to measure the deterioration of stone and to assess the effectiveness of treatment methods. Mater Struct 13(6):175–253
23. Verges-Belmin V (2001) Altération des pierres mises en œuvre. In ed Hermes, Géomécanique Environnementale. Risques Naturels et Patrimoine, Paris, pp 191–235
24. Weber J, Gadermayr N, Bayer K, Hughes D, Kozlowski R, Stillhammerova M et al (2007) Roman cement mortars in Europe's architectural heritage of the 19th century. J ASTM Int 4(8). doi:10.1520/JAI100667
25. Campbell DH (1999) Microscopical examination and interpretation of Portland cement and clinker, 2nd edn. Portland Cement Association, Skokie
26. Cailleux E, Marie-Victoire E, Sommain D, Brouard E (2005) Microstructure and weathering mechanisms of natural cements used in the 19th century in the French Rhône-Alpes region. In: Repair mortars for historic masonry RELIM workshop, Unedited pre-prints, Delft
27. Taylor HFW (1997) Cement chemistry, 2nd edn. Academic Press, London
28. Blezard RG (1998) The history of calcareous cements. In: Hewlett PC (ed) Lea's chemistry of cement and concrete, 4th edn. Arnold Publishers, London, pp 1–23
29. Vicat LJ (1858) Recherches sur les causes chimiques de la destruction des composés hydrauliques par l'eau de mer, et sur les moyens d'apprécier leur résistance à cette action, 2nd edn. Valmont, Paris
30. Sabbioni C, Zappia G, Riontinoa C, Blanco-Varela MT, Aguilera J et al (2001) Atmospheric deterioration of ancient and modern hydraulic mortars. Atmos Environ 35(3):539–548. doi:10.1016/S1352-2310(00)00310-1
31. Marion AM, Daube J, Smitz R (2001) The stability of pyrite in calcareous aggregate: investigations in old concrete structures. In: Proceedings of the 23rd international conference on cement microscopy, New Mexico, pp 146–164
32. Vallet JM, Gosselin C, Bromblet P, Rolland O, Verges-Belmin V, Kloppmann W (2006) Origin of salts in stone monument degradation using sulphur and oxygen isotopes: first results of the Bourges cathedral (France). J Geochem Explor 88(1–3):358–362